NeuroImage **14,** 1136–1149 (2001)
doi:10.1006/nimg.2001.0922, available online at http://www.idealibrary.com on IDEAL®

Rostrolateral Prefrontal Cortex Involvement in Relational Integration during Reasoning

Kalina Christoff,* Vivek Prabhakaran,† Jennifer Dorfman,‡ Zuo Zhao,* James K. Kroger,§ Keith J. Holyoak,¶ and John D. E. Gabrieli*

**Department of Psychology and †Program in Neurosciences, Stanford University, Stanford, California 94305; ‡Department of Psychology, Northwestern University, Evanston, Illinois 60208; §Department of Psychology, Princeton University, Princeton, New Jersey 08544; and ¶Department of Psychology and Brain Research Institute, University of California at Los Angeles, Los Angeles, California 90095*

Received March 22, 2001

Patient and neuroimaging studies indicate that complex reasoning tasks are associated with the prefrontal cortex (PFC). In this study, we tested the hypothesis that the process of relational integration, or considering multiple relations simultaneously, is a component process of complex reasoning that selectively recruits PFC. We used fMRI to examine brain activation during 0-relational, 1-relational, and 2-relational problems adapted from the Raven's Progressive Matrices and hypothesized that PFC would be preferentially recruited by the 2-relational problem type. Event-related responses were modeled by convolving a canonical hemodynamic response function with the response time (RT) associated with each trial. The results across different analyses revealed the same pattern: PFC activation was specific to the comparison between 2- and 1-relational problems and was not observed in the comparison between 1- and 0-relational problems. Furthermore, the process of relational integration was specifically associated with bilateral rostrolateral PFC (RLPFC; lateral area 10) and right dorsolateral PFC (areas 9 and 46). Left RLPFC showed the greatest specificity by remaining preferentially recruited during 2-relational problems even after comparisons were restricted to trials matched for RT and accuracy. The link between RLPFC and the process of relational integration may be due to the associated process of manipulating self-generated information, a process that may characterize RLPFC function. © 2001 Academic Press

INTRODUCTION

Patient studies have shown that the prefrontal cortex (PFC) is essential for the complex cognitive processes underlying reasoning and problem solving (e.g., Luria, 1966; Milner, 1963, 1964). Neuroimaging studies have supported this view by demonstrating PFC activation across many reasoning tasks (Berman *et al.*, 1995; Baker *et al.*, 1996; Nagahama *et al.*, 1996; Owen *et al.*, 1996; Goel *et al.*, 1997, 1998, 2000; Prabhakaran *et al.*, 1997, 2001; Rao *et al.*, 1997; Goldberg *et al.*, 1998; Osherson *et al.*, 1998; Ragland *et al.*, 1998; Dagher *et al.*, 1999; Goel and Dolan, 2000; Wharton *et al.*, 2000). Furthermore, several neuroimaging studies have shown that PFC activation increases as a consequence of increasing problem difficulty (Baker *et al.*, 1996; Owen *et al.*, 1996; Prabhakaran *et al.*, 1997; Dagher *et al.*, 1999).

There are at least two possible explanations regarding such prefrontal activations. One hypothesis is that they are due to the *longer duration of processing* associated with increasing problem difficulty. An alternative hypothesis is that prefrontal activations are due to *novel types of processes* invoked by specific reasoning demands.

In line with the second hypothesis, it has been proposed that PFC is essential for particular reasoning processes characterized by a requirement to consider multiple relations simultaneously (Robin and Holyoak, 1995). In general, the relational complexity of a problem (Halford and Wilson, 1980; Halford *et al.*, 1998) can be defined in terms of the number of related dimensions, or sources of variation, that need to be considered simultaneously in order to arrive at a correct solution. Halford *et al.* identified at least three levels of complexity: (i) 0-relational, in which no dimensional variation needs to be considered; (ii) 1-relational, in which a single dimension of variation needs to be considered at any moment of time; and (iii) 2-relational, in which two dimensions of variation need to be considered simultaneously and, therefore, integrated. The process of relational integration, or processing multiple relations simultaneously, is required only at the last, 2-relational level.

Relational integration appears to be a specific kind of mental computation that develops slowly in humans and so late in primate evolution as to be unique to humans. Children under 5 years of age can solve 0- and

1053-8119/01 $35.00

1-relational problems, but fail to solve 2-relational problems that demand integration of multiple relations, even when matched for working memory load to the 1-relational problems (Halford, 1984). Nonhuman primates can solve 1-relational problems, but cannot solve problems that require processing multiple relations simultaneously (reviewed in Tomosello and Call, 1997). Robin and Holyoak (1995) proposed that failures in relational integration may be attributable to the relatively slow frontal lobe maturation in humans (as indexed by myelination and other markers of cortical development) and to the great expansion of frontal cortex in human evolution. Such ontogenetic and phylogenetic developmental evidence supports the hypothesis that the PFC has a selective role in the process of relational integration.

To test this hypothesis, Waltz *et al.* (1999) examined the performance of patients with frontal variant of frontotemporal dementia during two tasks: a deductive reasoning task involving transitive inference and an inductive reasoning task involving problems adapted from the Raven's Progressive Matrices (RPM) test. For both tasks, patients performed at normal levels for 0-relational and 1-relational problems, but were impaired on 2-relational problems. These findings suggest that the ability to integrate multiple relations demands the integrity of PFC.

In this study, we used fMRI to examine brain activation in healthy volunteers during 0-relational, 1-relational, and 2-relational problems adapted from the RPM test. The relational complexity of each problem was defined as the number of relations that had to be considered simultaneously in order to solve the problem. Verbal protocol and eye-movement analyses have shown that RPM problems are solved using a sequential, reiterative strategy for inducing and encoding the rules or relationships of change within each problem (Carpenter *et al.*, 1990). Thus, the method we employed for defining the number of relations in each problem had been shown to be valid both psychologically (Carpenter *et al.*, 1990) and neuropsychologically (Waltz *et al.*, 1999).

Our goal was to test whether PFC has a selective role in the process of relational integration in healthy young volunteers and to determine whether specific PFC subregions mediate this role. We hypothesized that increases in PFC activation would be specific to the 2-relational problems and would be observed independently of increases in duration of processing. We used an event-related procedure that allowed randomized presentation of different problem types, so that participants were unable to anticipate what type of problem would be presented next. In addition, the duration spent working on each problem was recorded and used in modeling each event-related response. In this way, we were able to identify regions activated by novel processes separately from regions activated by longer engagement of processes common to solving all problem types.

MATERIALS AND METHODS

Participants

Ten right-handed volunteers from the Stanford community (6 female) took part in the experiment. Participants were 18 to 29 years of age (mean age 22.2) and were native speakers of English. Data from 2 additional participants were collected but excluded, one due to an unusually severe susceptibility-related signal dropout and the second due to technical problems with the presentation software. All participants gave informed, written consent to participate in the experiment. The study was approved by the Institutional Review Board at Stanford University.

Cognitive Task

Problems had the general form of the Raven's Progressive Matrices (Raven, 1938). Each problem consisted of a 3×3 matrix of figures, with the bottom right figure missing (Fig. 1). After considering the relationship among the given matrix figures, participants had to infer the missing figure and select it from among the four choice alternatives presented on the right side of the matrix.

Three different types of problems were created: 0-relational, 1-relational, and 2-relational. The 0-relational problems (Fig. 1a) involved no relationship of change and required no relational processing in order to be solved. The 1-relational problems (Fig. 1b) involved a change in either the horizontal or the vertical dimension and, therefore, required processing of a single relation. Finally, the 2-relational problems (Fig. 1c) involved two relations of change, in both the horizontal and the vertical direction. Inferring the correct answer required considering the converging change along both dimensions. Thus, the 2-relational problems required that two relations be integrated, or considered simultaneously.

Behavioral Procedure

The different problem types were presented in a pseudorandom order, consistent across participants. Each trial lasted 30 s and started with a visual cue (a 500 ms fixation cross) to alert participants to the beginning of a new trial (Fig. 2). After a 1500-ms period following the cue's offset, a problem appeared and participants started solving it. When ready, they pressed one of four buttons, indicating which figure they had selected as their answer. The time from the problem onset to the participant's response defined the response time (RT) for each trial. Problems were pretested so that none of them took more than 14 s to be solved, and

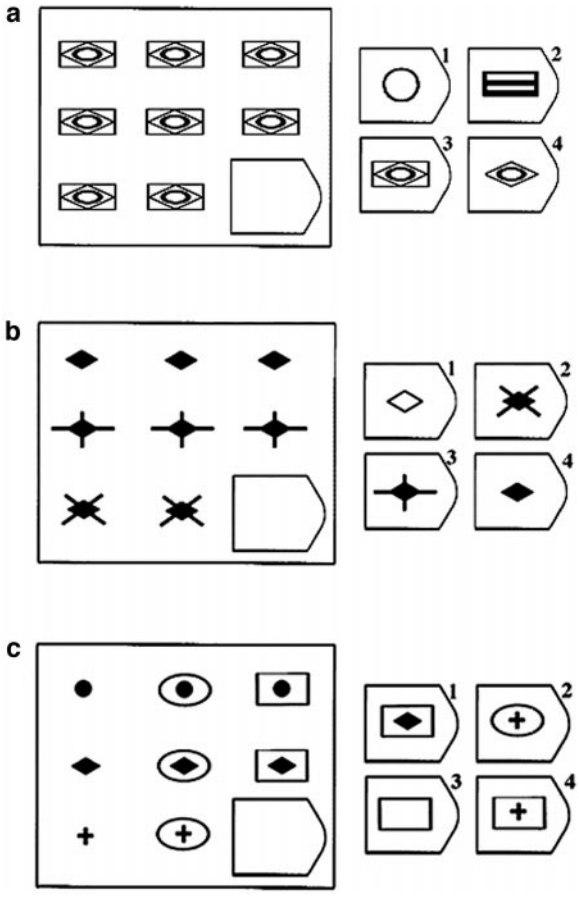

FIG. 1. Examples of problem types used in the experiment: (a) 0-relational, (b) 1-relational, and (c) 2-relational. Participants had to infer the missing figure and select it among the four choice alternatives. Correct answers for the examples given here are (a) 3, (b) 2, and (c) 4.

all responses during the experiment occurred within the response deadline (or 16 s after the problem onset). This allowed for at least 12 s of rest between problems—time necessary for the hemodynamic response to return to baseline before the next trial's onset. The instructions emphasized accuracy over speed of response, and participants were reminded to mentally rest in the period between their response and the next fixation cross.

Stimuli were generated from a computer and back-projected onto a screen located above the participant's head via a magnet-compatible projector. Visual images were viewed from a mirror mounted above the participant's head. Before scanning, participants were given brief practice on the RPM test (six problems total, two problems in each of the three conditions). During scanning, participants responded with their right hand, using their index, middle, ring, and small fingers to press one of four buttons on a hand-held button-box. The four keys corresponded to the four possible choice answers.

MRI Scanning Procedure

Imaging was performed using a 1.5 T whole-body MRI scanner (General Electric Medical Systems Signa, Rev. 5.5, Waukesha, WI). A top-hat elliptical quadrature birdcage head-coil was positioned around the participant's head to obtain the activation signal. Head movement was minimized using a bite-bar, formed with each participant's dental impression. Prior to functional imaging, 16 axial-oblique flow-compensated spin echo T1-weighted anatomic images [repetition time (TR) = 500 ms; minimum echo time (TE) = 40 ms; field of view (FOV) 20 × 20 cm^2; slice thickness 7 mm; in-plane resolution 3.125 mm] were acquired parallel to the anterior commissure/posterior commissure line. Following this, functional images were obtained (TR = 2000 ms; TE = 40 ms; flip angle 87°; FOV 20 × 20 cm^2; 64 × 64 voxels) in the same slice locations used for anatomic images. These functional images contained BOLD contrast intensity values and were acquired continuously during task performance. The volumes covered the whole brain (16 contiguous slices, each 7 mm thick; 1-interleaved) and were acquired using a T2*-weighted 2D gradient-echo spiral pulse sequence (Noll *et al.*, 1995; Glover and Lai, 1998), which is relatively insensitive to motion artifacts due to pulsatility (Glover and Lee, 1995). A total of 1080 functional volumes were acquired for each participant over 36 min (three sessions, 12 min each). Three discarded volumes (a total of 6 s) were acquired at the beginning of each session to allow for T1 stabilization. Finally, a high-resolution T1-weighted multislice anatomical image was acquired in axial orientation, using a 3D spoiled GRASS (SPGR) pulse sequence (TR = 50 ms; minimum TE; flip angle 15°; 124 contiguous slices of 1.5 mm thickness; 256 × 192 matrix; FOV 24 × 24 cm^2).

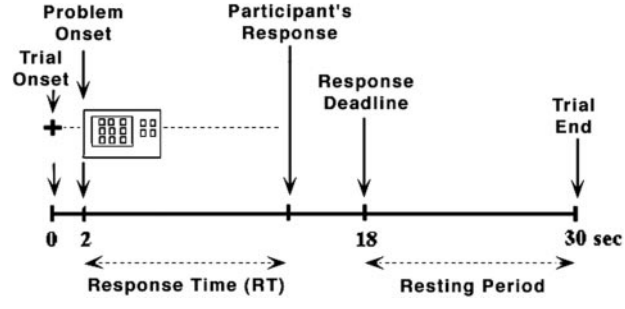

FIG. 2. Sequence of events within a trial. Each trial lasted 30 s and started with a fixation cue, followed by a problem's onset. The problem remained on the screen until the participant responded. The time from the problem onset to the participant's response defined the response time for each trial. All responses occurred before the response deadline, or within 16 s after the problem onset, thus allowing at least 12 s of rest between problems—time necessary for the hemodynamic response to return to baseline before the next trial's onset.

Data Preprocessing

Image reconstruction was performed offline by transferring the raw data to a Pentium II running RedHat 5.2 Linux (Red Hat, Inc., Durham, NC). Image preprocessing and statistical analysis were performed using SPM99b (Wellcome Department of Cognitive Neurology, http://www.fil.ion.ucl.ac.uk/spm). To account for the different sampling times of the different slices, voxel time series were interpolated using sinc interpolation and resampled using the first (bottom) slice as a reference point. All T2*-weighted volumes were realigned to the first one in the time series to correct for between-scan motion. The structural T1-weighted volumes were spatially normalized to a standard template (the MNI brain of Cocosco *et al.*, 1997) in the space of Talairach and Tournoux (1988) using a 12-parameter affine normalization and 12 nonlinear iterations with $7 \times 8 \times 7$ basis functions (Ashburner and Friston, 1999). The spatial transformations derived from normalizing the structural volume taken in the functional acquisition plane were applied to the realigned T2*-weighted volumes. After normalization, all volumes were resampled in $2 \times 2 \times 4$ mm voxels using sinc interpolation in space. Finally, all T2*-weighted volumes were smoothed with an 8-mm full width at half-maximum isotropic Gaussian kernel to compensate for residual between-subject variability after spatial normalization and permit application of Gaussian random field theory to provide for corrected statistical inference (Friston *et al.*, 1994).

Voxel-wise Analyses

Initial exploratory analyses were performed to assess the magnitude of pairwise differences between the different problem types at each voxel. As part of these analyses, two further preprocessing steps were performed using routines within SPM99b. First, to remove low-frequency drifts in the BOLD signal, data were high-pass filtered, using an upper cut-off period of 150 s, by constructing a convolution matrix for the first few basis functions of a one-dimensional discrete cosine transform. In addition, to remove effects due to global intensity fluctuations in the signal, data were proportionally scaled to a global mean of 100.

Condition effects at each voxel were estimated according to the general linear model (Friston *et al.*, 1995). The model included: (i) the observed time series of intensity values, representing the dependent variable; (ii) covariates modeling session-specific effects, later treated as confounds; and (iii) regressor functions constructed on the basis of a synthetic hemodynamic response function (HRF), modeling the hemodynamic response that would be expected to occur if a region is recruited by a particular problem type.

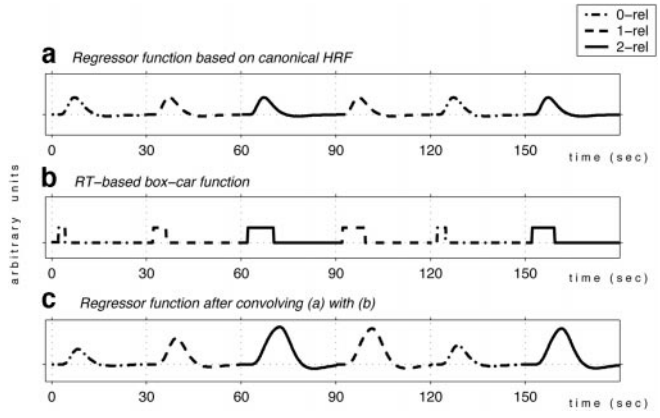

FIG. 3. Construction of regressor functions taking into account the different time participants spent working on the problem in each trial. (a) Regressor function based on the canonical hemodynamic response function (HRF) having a fixed shape, identical for each trial. (b) Boxcar function based on the participant's response time (RT) for each trial. (c) Regressor function resulting from convolving the HRF-based regressor in (a) with the RT-based boxcar function in (b). The shape of the response in (c) varies from trial to trial thus modeling increases in duration and amplitude of response that would be expected because of increased time spent working on a problem. *Note.* The regressor functions used to model the response at each voxel spanned the entire session length (360 s) while the figure illustrates only the first six trials of a session. In addition, the regressor functions were continuous with values corresponding to zero during trials in which problem types other than the type being modeled were presented. These zero values are omitted to make visual comparisons between the different regressors easier.

Fixed HRF Analysis

The traditional approach to constructing regressor functions for event-related analysis is to use an HRF of fixed duration and amplitude to model the BOLD response time-locked to the stimulus onset for each trial (Josephs *et al.*, 1997). This method, however, models responses in all trials as having the same shape (Fig. 3a). Although it is possible to include first-order time or dispersion derivatives in order to accommodate for small deviations in the shape of the hemodynamic response across trials (Friston *et al.*, 1998), when large differences in response duration are present, this method may not provide an appropriate model.

RT-Convolved HRF Analysis

Given that the period of time participants spent working on different trials varied extensively (RTs ranged approximately between 1 and 9 s, excluding responses that occurred more than 2 standard deviations away from the mean), we employed a modification of the above approach. For each participant, we constructed regressor functions that took into account the specific RT associated with each trial. Figure 3 illustrates the process of regressor construction for the first six trials of a session.

All constructed functions were continuous, with values corresponding to zero during trials in which problem types other than the types being modeled were presented. (These zero values are omitted from Fig. 3 to make visual comparisons between the different regressors easier.) First, nine regressors (3 conditions × 3 sessions) were constructed using the canonical HRF to model the occurrence of problems of each type, within each session (Fig. 3a). Second, nine analogous RT-based boxcar functions were constructed with values corresponding to 1 during the period between a problem's onset and the participant's response, and 0 otherwise (Fig. 3b). Finally, each of the canonical HRF regressors was convolved with the corresponding boxcar function. Convolution was done separately for each trial, using finite impulse response digital filtering as implemented in MATLAB5 (Mathworks, Inc., Sherborn, MA). The shape of the response in the resulting regressors (Fig. 3c) varied from trial to trial, thus modeling increases in duration and amplitude of response that would be expected because of increased duration of processing.

The model including these RT-based regressors was used to interrogate the data as a primary form of analysis. In addition, to ensure compatibility with previously reported neuroimaging studies of reasoning, we performed an analysis with regressors constructed by using a fixed HRF spanning a period of 16 s after each problem's onset (the maximum duration spent on an individual problem). The results from this latter analysis are briefly presented and later discussed in relation to the results from the primary analysis.

Regionally specific effects were estimated using linear contrasts to compare the parameter estimates for regressors modeling particular problem types. The two comparisons of interest were (i) 1-relational versus 0-relational problems and (ii) 2-relational versus 1-relational problems. Because the regressors in the primary analysis were constructed to take into account the duration of time spent working on each problem, these comparisons could be used to identify regions where the BOLD response increased above and beyond the increases attributable to duration of processing.

Contrasts were tested by a voxel-specific repeated-measures t test across participants, thus effecting a random effects model. The t maps were subsequently transformed to the unit normal Z distribution to create a statistical parametric map for each contrast. The areas reported below consist of voxels that survived a threshold of $P < 0.001$ ($Z > 3.09$) uncorrected for multiple comparisons.

The hypothesized differences between conditions concern differences due to greater *increase* in the evoked BOLD response between conditions (i.e., differential extent of response above baseline) and not differences due to greater *decrease* in BOLD response (i.e., differential extent of response below baseline). This distinction was necessary because, while event-related increases in BOLD response are known to be associated with neural activity, the physiological interpretation of event-related decreases in BOLD signal is still unclear and currently under investigation (e.g., Raichle, 1998; Raichle *et al.*, 2001). To identify only voxels showing significant increase in response above baseline, we created mask images for each of the problem types, containing voxels showing significant negative correlation with the regressors for this problem type. The threshold for these mask images was set at $P < 0.001$ (same as the activation threshold used to report results for the comparisons of interest), and they were applied to the analysis of reasoning-related brain activation to exclude areas in which the BOLD signal showed significant event-related decrease.

The foci of maximum activation were localized on a high-resolution anatomical image created by averaging the normalized individual high-resolution anatomical images. The locations of these maxima in terms of Brodmann areas (Brodmann, 1909) were determined using the nomenclature given by Talairach and Tournoux (1988), after adjustment for differences between the MNI and Talairach coordinate systems (http://www.mrc-cbu.cam.ac.uk/Imaging/mnispace.html).

Anatomical Regions of Interest (ROI) Analysis

In addition to the voxel-wise analysis, we conducted an independent analysis in anatomically defined ROIs for the PFC only. Thirty ROIs were defined (see Appendix) as regions of intersection between gyri and Brodmann areas (BAs) (see Fig. 5 for ROI outlines). The ROIs were constructed using labels from the Talairach Daemon database (http://ric.uthscsa.edu/projects/talairachdaemon.html) and were transformed into MNI space, as we have described elsewhere (Brett *et al.*, 2001). The raw signal intensities from all voxels within an ROI were averaged and the corresponding values were treated as a time series spanning the entire length of the experiment.

The time series derived from each ROI underwent a series of preprocessing steps to minimize noise-related components. First, to remove extreme values associated with scanner noise, outliers with an absolute Z score >2 were replaced with the trimmed mean for the time series. Second, session-specific grand mean scaling was applied by dividing the values within each session by the mean across this session and multiplying the resulting value by 100. Third, within-session linear detrending was performed by removing the best straight-line linear fit. Finally, a band-pass second-order Butterworth filter was designed and applied to the time series to reduce low-frequency confounds (by attenuating frequencies below 0.0156 Hz) and high-frequency noise (by attenuating frequencies above 0.0417 Hz).

TABLE 1

Mean Accuracy and Latency Data for the Different Conditions (±SE)

Problem type	Percentage correct	Response time (s)
0-relational	99.6 (±0.4)	2.78 (±0.25)
1-relational	96.7 (±1.2)	4.19 (±0.31)
2-relational	85.0 (±3.6)	5.66 (±0.36)

Note. Response time statistics are computed for accurate responses only. SE, standard error of the mean response across the 10 participants.

The time series was then separated into 30 s trial blocks containing the fMRI signal changes related to each problem's onset. The trial blocks corresponding to a particular problem type were treated as replications and were later trial-averaged to compare the hemodynamic response for different problem types within a given ROI. For reasons stated earlier, only those ROIs showing a nonnegative average response were used in subsequent analysis. No shifts were performed with respect to the value of the first point in the average time courses.

RESULTS

Behavioral Performance

Participants were highly accurate with 93.8% overall accuracy (accuracy and mean response time for each problem type are shown in Table 1). Increasing relational complexity resulted in reduced accuracy ($F[2,18] = 14.91$, $P < 0.001$) and slower latency of response ($F[2,18] = 124.96$, $P < 0.001$). One-tailed post hoc linear comparisons revealed that RTs were significantly longer for 2-relational than for 1-relational ($t = 3.19$, $df = 27$, $P < 0.001$) and for 1-relational than for 0-relational problems ($t = 3.17$, $df = 27$, $P < 0.001$). Accuracy was significantly lower for 2-relational than for 1-relational problems ($t = 3.69$, $df = 27$, $P < 0.001$) and tended to be lower for 1-relational than for 0-relational problems ($t = 0.92$, $df = 27$, $P = 0.09$).

Neuroimaging Results

Voxel-Wise Analysis

RT-convolved HRF. The activation maxima from the primary analysis using RT-convolved HRF are given in Table 2 and are illustrated in Fig. 4a. No voxels surviving the $P < 0.001$ ($Z > 3.09$) threshold at the voxel level were revealed in the 1-relational vs 0-relational comparison. Two small clusters in the promotor cortex approached significance when the voxel threshold was relaxed to $P < 0.01$, but there were no PFC differences even at this level.

The 2-relational vs 1-relational comparison yielded activation in the PFC bilaterally. There were two left-lateralized cortical regions of activation. The first was a cluster in the left posterior and promotor PFC, extending over the inferior prefrontal and precentral gyri, including BA 44 and 6. The second cluster was located in the left anterior PFC, extending over the rostrolateral prefrontal cortex (RLPFC), including the lateral portion of BA10. The activation maxima in both of these left PFC regions survived correction for multiple comparison (correction was performed using a mask of all prefrontal cortex voxels showing significant main effect of reasoning).

TABLE 2

Maxima of Regions Showing Significant Signal Changes in a Voxel-wise Analysis Using RT-Convolved HRF

Region of activation	L/R	BA	No. of voxels	Talairach coordinates			*Z* value	*P* value
				x	*y*	*z*		
1-relational vs 0-relational								
no significant differences	—	—	—	—	—	—	—	—
2-relational vs 1-relational								
Inferior frontal gyrus	L	44	40 (167)	−44	4	33	3.65	<0.05*
Precentral gyrus	L	6		−38	0	37	3.59	<0.001
Middle frontal gyrus	L	10	2 (17)	−34	50	9	3.33	<0.05*
Head of caudate	L	—	48 (76)	−14	2	4	4.62	<0.001
Middle frontal gyrus	R	46	5 (40)	38	26	13	3.48	<0.001
Middle frontal gyrus	R	9	1 (24)	28	8	36	3.12	<0.001
Head of caudate	R	—	17 (61)	10	6	4	4.35	<0.001

Note. Activation maxima for voxels surviving $P < 0.001$ ($Z > 3.09$) are reported. The number of voxels per cluster at this threshold is given, followed by the number of voxels (in parentheses) surviving at $P < 0.005$ ($Z > 2.59$). Asterisks indicate significance values surviving correction for multiple comparisons. Where the cluster encompassed more than one region (either BA or gyrus), more than one activation foci are reported for representativeness. Talairach coordinates have been adjusted for differences between the MNI and the Talairach coordinate system (http://www.mrc-cbu.cam.ac.uk/Imaging/mnispace.html). Abbreviations: L, left; R, right; BA, Brodmann area.

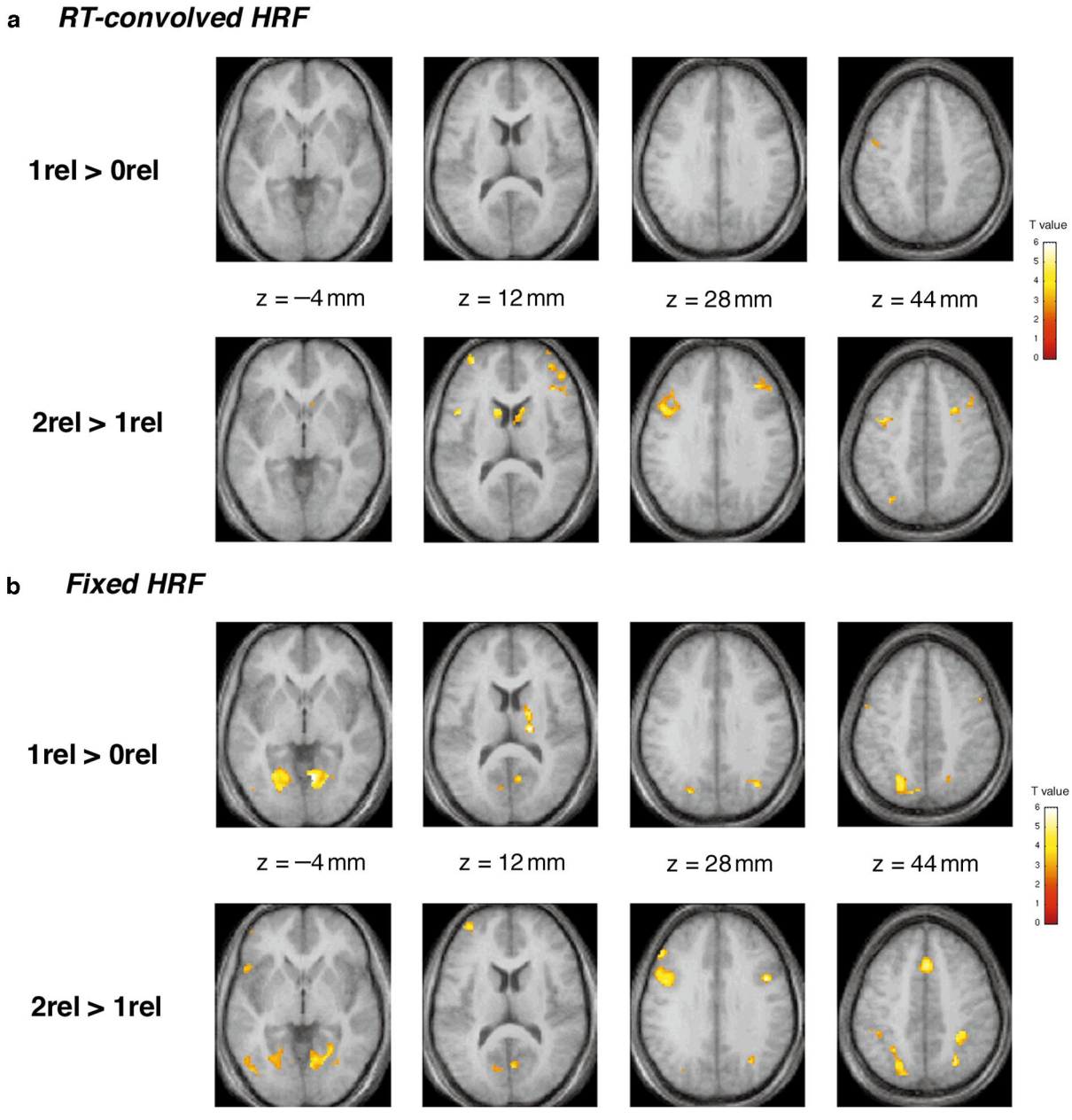

FIG. 4. Results from voxel-wise analysis (a) using RT-convolved HRF and (b) using fixed HRF. Regions showing significant increase in event-related response across all participants for the two main comparisons of interest. The results are rendered on axial slices of the group mean anatomical image, created by averaging the normalized individual high-resolution anatomical images. Results are thresholded at $P < 0.01$ uncorrected for multiple comparisons, with an extent threshold of 5 voxels. Details on individual maxima of activation for (a) are given in Table 2. Individual maxima of activation for (b) are discussed in the text (see Results). Abbreviations: 0rel, 0-relational; 1rel, 1-relational; 2rel, 2-relational.

The right-lateralized regions of activation for this comparison included the dorsolateral prefrontal cortex (DLPFC), including BA 9 and 46, with maxima of activation in the middle frontal gyrus (MFG). At a lower threshold level ($P < 0.01$), the two clusters merged into a single large right PFC cluster of activation, extending in anterior direction to include the RLPFC (lateral BA10).

In addition to PFC activations, the 2-relational vs 1-relational comparison yielded robust activation in the head of the caudate nucleus bilaterally. No other suprathreshold activations were observed for this comparison.

Fixed HRF. Comparing 1-relational vs 0-relational problems by using fixed HRF (Fig. 4b) revealed no suprathreshold PFC activations. There was bilateral activation in the extrastriate visual cortex (fusiform and lingual gyri, BA19), left lateralized activation in the superior parietal lobule (BA7), and a cluster of activation in the right thalamus. Activations in bilat-

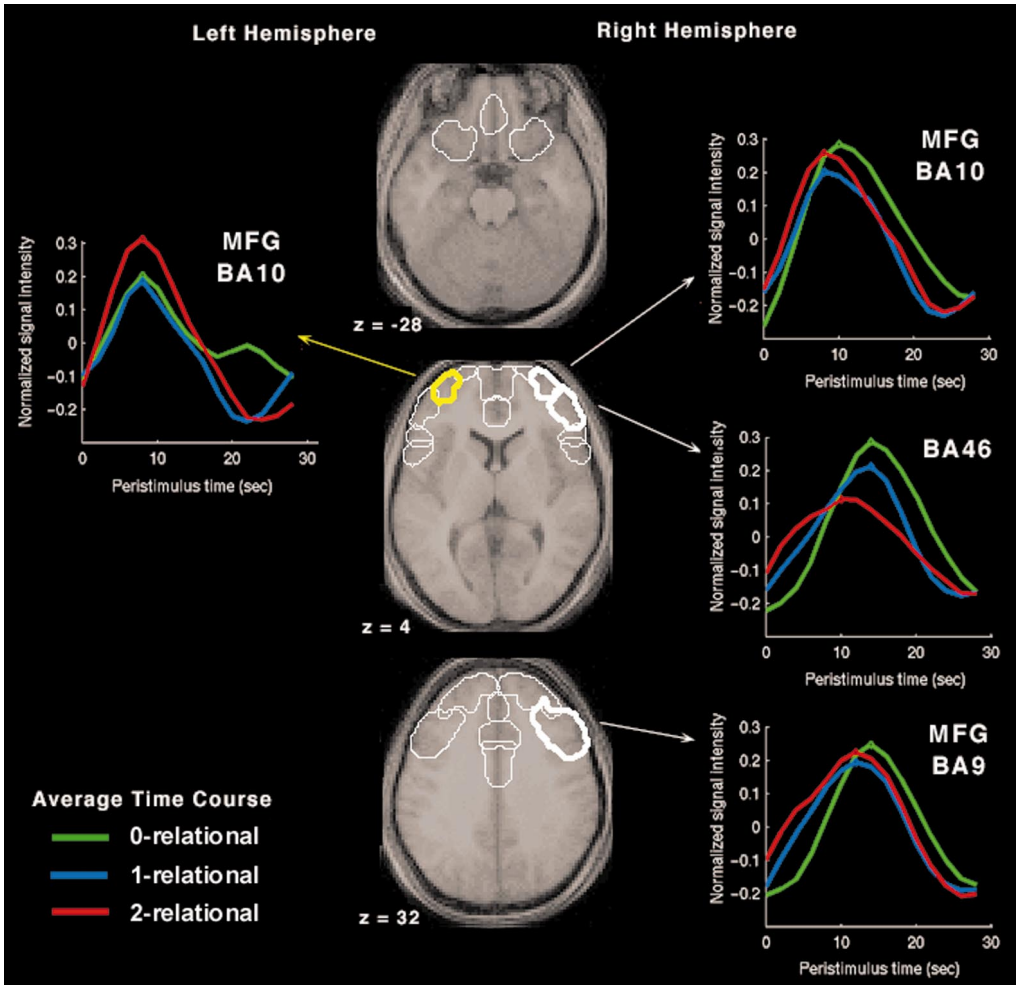

FIG. 5. Anatomical ROI analysis on trials matched for RT and accuracy (see Table 3 for statistics for the RT distributions across problem types). The event-related plots show the average time course for different problem types. Yellow contour indicates the ROI (left RLPFC) that preserved a pattern of significant differential response consistent with the pattern observed in the ROI analysis including all trials. Bold white contour indicates the ROIs (right RLPFC and the ROIs comprising the right DLPFC) that showed the predicated pattern of differential response when analysis was performed on all trials, but did *not* show such pattern when comparisons were restricted to RT-matched trials. Outlines of all other anatomical ROIs in prefrontal cortex are also shown (see Appendix for a list of all ROIs). All contours have been overlaid on axial slices of a subject-averaged T1-weighted anatomical image. Statistical significance was assessed by a signed-order pair-wise Wilcoxon test at the response peaks (see Results for more details). Peak response points are indicated with circles. Abbreviations: BA, Brodmann area; MFG, middle frontal gyrus.

eral extrastriate cortex and superior parietal lobule were also observed in the 2-relational vs 1-relational comparison. In addition, this second comparison revealed activations in left DLPFC (middle frontal gyrus, BA46) and left RLPFC (middle and superior frontal gyri, BA10), as well as bilateral activation in the inferior frontal gyrus (BA44 and 6) and a medial cluster of activation in the cingulate gyrus (BA32).

Anatomical ROI Analysis

Differential responses among problem types: all trials. The peak values from all trial-related evoked responses were used to perform a repeated measures F test, with participants treated as a random variable and different responses within each problem type treated as replications. Five anatomical ROIs (left BA10–MFG, left BA44, right BA10–MFG, right BA9–MFG, and right BA46) overlapped with or included regions activated in the primary voxel-wise analysis. The main effect of problem type in four of these five anatomical ROIs reached or approached significance at the $P < 0.05$ level: left BA10–MFG ($P < 0.05$, $F[2,18] = 4.26$), right BA10–MFG ($P < 0.01$, $F[2,18] = 6.25$), right BA46 ($P = 0.07$, $F[2,18] = 3.01$), and right BA9–MFG ($P = 0.07$, $F[2,18] = 3.17$). The response in the remaining 25 PFC ROIs (see Appendix) did not reveal a main effect of problem type, a finding consistent with the results from the voxel-wise analysis. Post hoc lin-

TABLE 3

Response Time Distribution Statistics for the RT-Matched Trials

Problem type	Mean (s)	Median (s)	Standard deviation (s)
0-relational	4.05	4.01	0.68
1-relational	4.07	4.08	0.70
2-relational	4.07	4.03	0.66

Note. A total of 108 correctly answered trials were selected, 36 for each problem type.

ear comparisons between problem types were performed on the peak values in each of the four ROIs approaching or showing significant main effect. The results were again consistent with the pattern observed in the voxel-wise analysis; 2-relational problems were associated with higher peaks than both 1-relational and 0-relational problems and there was no significant difference between 1-relational and 0-relational problems.

Differential responses among problem types: RT-matched trials. Differences in peaks across problem types may be driven not only by increases in relational complexity, but also by increases in other sources of difficulty (e.g., visuospatial complexity of processing). To try to separate the effects of increasing relational complexity from the effects of other sources of difficulty, we selected 108 trials so that they formed 36 RT-matched triplets, each containing one trial for every one of the three problem types. All trials within a triplet were selected from the same subject and corresponded to problems that were answered correctly with roughly equal RT. This resulted in three groups of problems equated for overall level of difficulty in terms of RT and accuracy. Statistics for the RT distributions across problem types are given in Table 3. In addition, problems were selected so that within each group they had a counterbalanced history; i.e., each problem type was preceded by all different problem types in equal proportion. This was necessary in order to eliminate differences between problem types that may be caused by residual lag of hemodynamic response from preceding trials. For each of the four ROIs approaching or showing significant main effect of problem type, the peaks of responses were compared across problem types, to find out if the effect of increasing relational complexity is preserved after equating for accuracy and RT.

The average time courses across problem types are shown in Fig. 5. To test for differences in activation, we performed a nonparametric analysis using the signed-order Wilcoxon test for pairwise differences between groups. In left BA10–MFG, the previously observed pattern was preserved: 2-relational problems yielded higher peaks than both 1-relational ($T = 227$, $n = 36$, $P < 0.05$, one-tailed) and 0-relational ($T = 158$, $n = 36$, $P < 0.005$, one-tailed), whereas 1-relational and 0-relational did not differ. In the three right PFC ROIs, however, this pattern was not preserved. In right BA10–MFG, 2-relational problems yielded significantly higher peaks than 1-relational ($T = 201$, $n = 36$, $P < 0.05$, one-tailed), but 0-relational were not significantly different from any of the other two types. In right BA9–MFG, there were no significant differences among problem types. Similarly, in right BA46, there were no significant differences, except for a difference between 0-relational and 2-relational problems that reached significance, but in the opposite of the expected direction (0-relational higher than 2-relational, $T = 218$, $n = 36$, $P < 0.05$, one-tailed).

DISCUSSION

The results across different analyses revealed the same pattern: PFC activation was specific to the comparisons between 2- and 1-relational problems and was not observed in the comparisons between 1- and 0-relational problems. In left RLPFC, this pattern continued to hold even after equating for RT and accuracy among problem types. These results converge with the patient findings by Waltz *et al.* (1999) and support the hypothesis that PFC is selectively involved during the process of relational integration. The results are also consistent with the view that PFC is preferentially engaged during relationally complex processes (Robin and Holyoak, 1995) and confirm that, as proposed by Halford *et al.* (1998), the relational complexity of a task can be successfully used to predict PFC recruitment.

One of the main goals of the present study was to identify regions activated by novel reasoning processes separately from regions activated by increased duration of processes shared among conditions. This distinction was important, because the comparisons between problem types were designed hierarchically so that each condition required processing an additional relation. This parametric increase in relational complexity was inherently associated with an overall increase in processing duration.

Several aspects of the present results point to the fact that the PFC activations observed in the comparison between 2- and 1-relational problems were associated with a novel reasoning process, rather than increased duration of processing. First, although there were virtually identical increases in processing duration between 1- and 0-relational and between 2- and 1-relational problems, as measured by response latencies, PFC activations were not observed for the comparison between 1- and 0-relational problems. Instead, these activations were found only in the comparison between 2- and 1-relational problems, when the process of relational integration was introduced. Second, the analysis using RT-convolved HRF revealed that

PFC regions activated in the comparisons between 2- and 1-relational problems increased in response beyond the increase that would be expected from differences in duration of processing alone. Third, at least one PFC region, left RLPFC, remained activated even after comparisons were restricted to trials matched for accuracy and RT among problem types. Together, these results strongly argue that the observed PFC activations were associated with a novel process specifically recruited during 2-relational problems, rather than with the associated increase in processing duration.

Novel Types of Processes vs Longer Duration of Processing

Distinguishing between these two sources of activation is a widespread issue that has received only limited attention in the neuroimaging literature so far. In general, when interpreting the results from comparisons based on the cognitive subtraction principle, activations are frequently assumed to reflect a novel process unique to one of the conditions. If there is a systematic difference in response latency between conditions, however, it may also contribute to the activation pattern—a contribution that may reflect not a novel process, but instead, a longer engagement of the same processes. D'Esposito *et al.* (1997) discussed this problem in the context of blocked design studies and emphasized the importance of considering the spacing between trials within a block when interpreting activations. They proposed that activations can be interpreted by comparing the results from a fixed-paced experiment with the results from the same experiment repeated under self-paced conditions.

The RT-convolution method presented here may allow for such discrimination in the context of event-related observations, by comparing the results from different types of analyses performed on a given data set. In the present study, significant differences in PFC regions were revealed both by the analysis using RT-convolved HRF and by the analysis using fixed HRF. On the other hand, activations in posterior cortical regions, including extrastriate visual cortex and superior parietal lobule, were observed only in the analysis using fixed HRF. This suggests that these posterior activations reflect increases that can be fully accounted for by the increase in duration of processing. We therefore interpret these activations as reflecting longer engagement of processes shared among conditions (e.g., visual inspection or attentional engagement). The prefrontal activations identified by the RT-convolved HRF analysis, on the other hand, reflected increase in response exceeding the increase that would be expected from differences in duration of processing alone. We therefore interpret these prefrontal activations as reflecting a novel process, the process of relational integration, uniquely engaged by the 2-relational problem type. The analysis using RT-convolved HRF also revealed right PFC and caudate activations that were not observed in the fixed-HRF analysis, a difference that may be attributable to an improved sensitivity of the RT-convolved HRF analysis, resulting from incorporating knowledge about processing duration in the model of each event-related response.

Both the event-related method presented here and the blocked design method described by D'Esposito *et al.* (1997) rely on the assumption that an increase in duration of processing is linearly related to a corresponding increase in BOLD signal. The relationship between duration of processing and neuroimaging signal has been investigated for several primary cortical regions and a linear relationship has been found to provide a good approximation (Boynton *et al.*, 1996; Cohen, 1997). Some nonlinearities, however, have been observed for processing durations of roughly 3 s or shorter (Boynton *et al.*, 1996; Vazquez and Noll, 1998; Glover, 1999). Approximately 35% of the responses in the present study occurred within 3 s from the problem's onset. The general pattern of PFC activation, however, remained consistent among the RT-convolved HRF, the fixed HRF, and the anatomical ROI analysis including all trials, suggesting that none of these analyses were differentially influenced by nonlinear effects.

Prefrontal and Subcortical Involvement in Complex Reasoning

In the present study, complexity-dependent increases in activation exceeding the effects of processing duration were observed only for PFC, suggesting that this may be the only cortical region sensitive to increasing reasoning complexity. Similar PFC specificity was noted by Dagher *et al.* (1999), who used the Tower of London, a reasoning task in which complexity can be defined as the minimum number of moves needed to arrive at a correct solution (Owen *et al.*, 1990). Dagher *et al.* found that performance of the Tower of London recruited a widely distributed network of prefrontal, visual, and parietal regions, but that task complexity correlated only with PFC activation. The present study supports the view that such PFC activation reflects reasoning complexity rather than the longer duration associated with additional moves.

The only other brain structure that revealed an effect of increasing reasoning complexity in both the present study and the study reported by Dagher *et al.* (1999) was the caudate nucleus. The caudate is anatomically related to PFC through multiple frontostriatal connections (Alexander *et al.*, 1986), and caudate lesions are known to produce specific impairments in complex reasoning processes such as planning, organizing, and sequencing (Mendez *et al.*, 1989; Petty *et al.*, 1996). Similar deficits in complex reasoning also occur in caudate-lesioned animals (Divac *et al.*, 1967;

Van den Bercken and Cools, 1982) and in early Huntington's disease (Caine *et al.*, 1978; Singh *et al.*, 1992), a disorder whose primary pathology involves the caudate nuclei. Neuroimaging studies have demonstrated caudate activation for multiple reasoning tasks (Owen *et al.*, 1996; Rao *et al.*, 1997; Goldberg *et al.*, 1998; Goel *et al.*, 2000; Osherson *et al.*, 1998; Dagher *et al.*, 1999). Thus, there is converging evidence that the PFC and the caudate are major components of a neural system mediating complex reasoning.

Relational Complexity and Prefrontal Function

In addition to reasoning, prefrontal cortex activation has been associated with a variety of complex cognitive functions, such as planning (e.g., Baker *et al.*, 1996), management of dual tasks (D'Esposito *et al.*, 1995), and working memory (e.g., Cohen *et al.*, 1997). Many of these tasks involve relational processing. Thus, complex planning requires working with multiple subgoals and organizing them in a subgoal hierarchy (Carpenter *et al.*, 1990; Shallice and Burgess, 1991). Building an optimal subgoal hierarchy would require considering multiple subgoal relations simultaneously (Halford *et al.*, 1998). Similarly, dual tasks require executing two action sequences in parallel. The management of dual tasks, therefore, would demand the integration of the temporal relations between these action sequences.

Likewise, working memory tasks often require participants to integrate multiple relations, such as the relative temporal or spatial order among stimuli. Variations in complexity of processing during the *n*-back task, for instance, can be defined in terms of processing relations between items in time (Waltz *et al.*, 1999). Identifying the item that is "one-back" requires processing of a single relation, while identifying the item that is "two-back" requires integration of two temporal relations. Thus, relational processes and, in particular, complex relational processes, such as relational integration, occur in a wide range of tasks that depend on PFC. The integration of relations, therefore, may be one of the common factors linking diverse prefrontal functions, such as planning, reasoning, and working memory.

Prefrontal Subregions Involved in Relational Integration

The present results converge with the patient findings by Waltz *et al.* (1999) and recent neuroimaging findings by Kroger *et al.* (in press), suggesting that relational integration may be one of the specific component processes of reasoning that are invoked with increasing problem difficulty and lead to PFC recruitment. Furthermore, our results extend the patient findings by identifying specific PFC subregions: Relational integration was associated with bilateral RLPFC and right DLPFC activations, although left RLPFC showed the greatest specificity by preserving its sensitivity to relational integration even after restricting comparisons to trials matched for RT and accuracy. On the other hand, the fact that RT matching eliminated the effect of relational complexity in right RLPFC and right DLPFC implies that these two regions may be sensitive not only to relational integration, but also to other processes influencing problem difficulty.

The analysis based on RT matching had several limitations. Selection was performed post hoc, based on dependent measures. Given the systematic increase in response latencies across problem types, the 0- and 2-relational problems selected by RT matching were most likely unrepresentative for their type and may have been associated with atypical recruitment of processes. In addition, this analysis had a diminished statistical power due to the limited number (36) of trials per problem type. Given this, it is striking that left RLPFC remained sensitive to the process of relational integration even after RT matching, in a situation in which the effects of increasing relational complexity were most likely counteracted by the effects of other factors influencing problem difficulty. This implies that relational integration may be one of the specific processes characterizing left RLPFC.

RLPFC and Complex Cognition

RLPFC activations have been observed during highly complex tasks across a wide range of domains. Based on a review of studies reporting activation in this region (Christoff and Gabrieli, 2000), we have proposed that it may be selectively involved in active processing, such as manipulation or evaluation, performed upon self-generated information. The present findings bear interesting implications relating to this hypothesis. First, they are consistent with it: The relational information associated with a problem from the RPM test is not given in the problem, but has to be inferred, or self-generated, on the basis of given information (the individual object features such as shape, texture, and size). The observed link between RLPFC activation and the process of relational integration, therefore, could be due to the associated process of manipulating the self-generated information about the change among objects.

Second, our results suggest the presence of a hemispheric asymmetry within the RLPFC. The majority of reported RLPFC activations have been right lateralized and are most consistently observed during tasks involving episodic retrieval (Cabeza and Nyberg, 2000). In the present study, however, RLPFC activation was left lateralized. In general, reasoning tasks involving relational inferences have been associated with exclusively left lateralized pattern of PFC activation. Thus, Wharton *et al.* (2000) used an analogical reasoning task that involved matching relations be-

tween items; they found activation in multiple left PFC regions, including RLPFC, but no activation in right PFC. Similarly, Goel *et al.* (1998) used a reasoning task, involving deductive relational inferences and, again, observed exclusively left-lateralized pattern of PFC activation. None of these studies, however, have focused on the RLPFC specifically, while our results bear direct implications for the functions of this prefrontal subregion. We propose that while right RLPFC may be preferentially involved in the evaluation of self-generated information (Christoff *et al.*, 2001), left RLPFC may be involved in manipulating self-generated information for the purposes of further abstracting new information. Such functional role would be consistent with the present results demonstrating specific involvement of left RLPFC in the process of relational integration.

The precise functions of the RLPFC, as well as the presence and nature of hemispheric specialization within it, remain objects of further discussion. It is likely, however, that this region plays a central role in complex cognitive processes. Therefore, elucidating its functions further may prove crucial for understanding the neural basis of reasoning.

APPENDIX

A List of the Prefrontal Anatomical ROIs Used in the ROI-Based Analysis, with Their Volumetric Size in Cubic Centimeters

Region	Volume (cm^3)
Left hemisphere	
BA8, middle frontal gyrus	7.9
BA8, superior frontal gyrus	7.8
BA9, middle frontal gyrus	7.8
BA9, superior frontal gyrus	6.0
BA10, middle frontal gyrus	6.8
BA10, superior frontal gyrus	9.6
BA11, orbitofrontal and middle frontal gyri	4.3
BA11, superior frontal gyrus	3.6
BA44, inferior frontal gyrus	2.9
BA45, inferior frontal gyrus	3.8
BA46, middle and inferior frontal gyri	8.8
BA47, inferior frontal gyrus	12.1
Right hemisphere	
BA8, middle frontal gyrus	7.6
BA8, superior frontal gyrus	7.8
BA9, middle frontal gyrus	8.6
BA9, superior frontal gyrus	6.5
BA10, middle frontal gyrus	7.8
BA10, superior frontal gyrus	9.7
BA11, orbitofrontal and middle frontal gyri	3.5
BA11, superior frontal gyrus	3.6
BA44, inferior frontal gyrus	2.7
BA45, inferior frontal gyrus	3.7
BA46, middle and inferior frontal gyri	9.2
BA47, inferior frontal gyrus	11.5
Medial	
BA9–8, medial frontal gyrus	10.5
BA10, medial frontal gyrus	9.9
BA11, medial frontal and rectal gyri	9.2
BA24–32, anterior cingulate	15.2
BA24, cingulate gyrus	13.7
BA32, cingulate gyrus	8.4

Note. BA, Brodmann area.

ACKNOWLEDGMENTS

Support for the research reported herein came from grants from the National Institute of Aging (NIAC-AG12995 and NIAC-AG112) to J.D.E.G. and a Stanford New Democracy Fellowship Award to K.C. We thank Shelley Zulman and Courtney Dirksen for help in preparing the stimuli, Amy Shelton for advice on statistical issues, and Matthew Brett for help on the Talairach to MNI transform used in ROI definition and for developing the slice display routine used in creating Fig. 5. We are also grateful to Lera Boroditsky, Boicho Kokinov, and three anonymous reviewers, for providing thoughtful remarks and suggestions regarding earlier versions of the manuscript.

REFERENCES

Alexander, G. E., DeLong, M. R., and Strick, P. L. 1986. Parallel organization of functionally segregated circuits linking basal ganglia and cortex. *Annu. Rev. Neurosci.* **9:** 357–381.

Ashburner, J., and Friston, K. J. 1999. Nonlinear spatial normalization using basis functions. *Hum. Brain Mapp.* **7:** 254–266.

Baker, S. C., Rogers, R. D., Owen, A. M., Frith, C. D., Dolan, R. J., Frackowiak, R. S. J., and Robbins, T. W. 1996. Neural systems engaged by planning: A PET study of the Tower of London task. *Neuropsychologia* **34:** 515–526.

Berman, K. F., Ostrem, J. L., Randolph, C., Gold, J., Goldberg, T. E., Coppola, R., Carson, R. E., Herscovitch, P., and Weinberger, D. R. 1995. Physiological activation of a cortical network during performance of the Wisconsin Card Sorting Test: A positron emission tomography study. *Neuropsychologia* **33:** 1027–1046.

Boynton, G. M., Engel, S. A., Glover, G. H., and Heeger, D. J. 1996. Linear systems analysis of functional magnetic resonance imaging in human V1. *J. Neurosci.* **16:** 4207–4221.

Brett, M., Christoff, K., Cusak, R., and Lancaster, J. 2001. Using the Talairach atlas with the MNI template. *NeuroImage* **13:** S85.

Brodmann, K. 1908. Beitraege zur histologischen Lokalisation der Grosshirnrinde. VI Mitteilung. Die Cortexgliederung des Menschen. *J. Psychol. Neurol.* **10:** 213–246.

Cabeza, R., and Nyberg, L. 2000. Imaging cognition. II. An empirical review of 275 PET and fMRI studies. *J. Cognit. Neurosci.* **12:** 1–47.

Caine, E., Hunt, R., Weingartner, H., and Ebert, M. 1978. Huntington's dementia: Clinical and neuropsychological features. *Arch. Gen. Psychiatry* **35:** 377–384.

Carpenter, P. A., Just, M. A., and Shell, P. 1990. What one intelligence test measures: A theoretical account of the processing in the Raven Progressive Matrices Test. *Psychol. Rev.* **97:** 404–431.

Christoff, K., and Gabrieli, J. D. E. 2000. The frontopolar cortex and human cognition: Evidence for a rostrocaudal hierarchical organization within the human prefrontal cortex. *Psychobiology* **28:** 168–186.

Christoff, K., Geddes, L. P. T., and Gabrieli, J. D. E. 2001. Rostrolateral prefrontal cortex involvement in evaluating self-generated information. *NeuroImage* **13:** S649.

Cocosco, C., Kollokian, V., Kwan, R., and Evans, A. 1997. Brainweb: Online interface to a 3D MRI simulated brain database. *NeuroImage* **5:** 425.

Cohen, M. S. 1997. Parametric analysis of fMRI data using linear systems methods. *NeuroImage* **6:** 93–103.

Cohen, J. D., Perlstein, W. M., Braver, T. S., Nystrom, L. E., Noll, D. C., Jonides, J., and Smith, E. E. 1997. Temporal dynamics of brain activation during a working memory task. *Nature* **386:** 604–608.

Dagher, A., Owen, A. M., Boecker, H., and Brooks, D. J. 1999. Mapping the network for planning: A correlational PET activation study with the Tower of London task. *Brain* **122:** 1973–1987.

D'Esposito, M., Detre, J. A., Alsop, D. C., Shin, R. K., Atlas, S., and Grossman, M. 1995. The neural basis of the central executive system of working memory. *Nature* **378:** 279–281.

D'Esposito, M., Zarahn, E., Aguirre, G. K., Shin, R. K., Auerbach, P., and Detre, J. A. 1997. The effect of pacing of experimental stimuli on observed functional MRI activity. *NeuroImage* **6:** 113–121.

Divac, I., Rosvold, H. E., and Szwarcbart, M. K. 1967. Behavioral effects of selective ablation of the caudate nucleus. *J. Comp. Physiol. Psychol.* **63:** 184–190.

Friston, K. J., Worsley, K. J., Frackowiak, R. S. J., Mazziotta, J. C., and Evans, A. C. 1994. Assessing the significance of focal activations using their spatial extent. *Hum. Brain Mapp.* **1:** 210–220.

Friston, K. J., Holmes, A. P., Worsley, K. J., Poline, J. P., Frith, C. D., and Frackowiak, R. S. J. 1995. Statistical parametric maps in functional imaging: A general linear approach. *Hum. Brain Mapp.* **2:** 189–210.

Friston, K. J., Fletcher, P., Josephs, O., Holmes, A., Rugg, M. D., and Turner, R. 1998. Event-related fMRI: Characterizing differential responses. *NeuroImage* **7:** 30–40.

Glover, G. H. 1999. Deconvolution of impulse response in event-related BOLD fMRI. *NeuroImage* **9:** 416–429.

Glover, G. H., and Lai, S. 1998. Self-navigated spiral fMRI: Interleaved versus single-shot. *Magn. Reson. Med.* **39:** 361–368.

Glover, G. H., and Lee, A. T. 1995. Motion artifacts in fMRI: Comparison of 2DFT with PR and spiral scan methods. *Magn. Reson. Med.* **33:** 624–635.

Goel, V., Gold, B., Kapur, S., and Houle, S. 1997. The seats of reason? An imaging study of deductive and inductive reasoning. *NeuroReport* **8:** 1305–1310.

Goel, V., Gold, B., Kapur, S., and Houle, S. 1998. Neuroanatomical correlates of human reasoning. *J. Cognit. Neurosci.* **10:** 293–302.

Goel, V., Buchel, C., Frith, C., and Dolan, R. J. 2000. Dissociation of mechanisms underlying syllogistic reasoning. *NeuroImage* **12:** 504–514.

Goel, V., and Dolan, R. J. 2000. Anatomical segregation of component processes in an inductive inference task. *J. Cognit. Neurosci.* **12:** 110–119.

Goldberg, T. E., Berman, K. F., Fleming, K., Ostrem, J., Van Horn, J. D., Esposito, G., Mattay, V. S., Gold, J. M., and Weinberger, D. R. 1998. Uncoupling cognitive workload and prefrontal cortical physiology: A PET rCBF study. *NeuroImage* **7:** 296–303.

Halford, G. S. 1984. Can young children integrate premises in transitivity and serial order tasks? *Cognit. Psychol.* **16:** 65–93.

Halford, G. S., and Wilson, W. H. 1980. A category theory approach to cognitive development. *Cognit. Psychol.* **12:** 356–411.

Halford, G. S., Wilson, W. H., and Phillips, S. 1998. Processing capacity defined by relational complexity: Implications for comparative, developmental, and cognitive psychology. *Behav. Brain Sci.* **21:** 803–831.

Josephs, O., Turner, R., and Friston, K. 1997. Event-related fMRI. *Hum. Brain Mapp.* **5:** 243–248.

Koechlin, E., Basso, G., Pietrini, P., Panzer, S., and Grafman, J. 1999. The role of the anterior prefrontal cortex in human cognition. *Nature* **399:** 148–151.

Kroger, J. K., Saab, F. W., Fales, C. L., Bookheimer, S. Y., Cohen, M. S., and Holyoak, K. J. Recruitment of anterior dorsolateral prefrontal cortex in human reasoning: A parametric study of relational complexity. *Cerebral Cortex*, in press.

Luria, A. R. 1966. *Higher Cortical Functions in Man*. Tavistock, London.

Mendez, M. F., Adams, N. L., and Lewandowski, K. S. 1989. Neurobehavioral changes associated with caudate lesions. *Neurology* **39:** 349–354.

Milner, B. 1963. Effects of different brain lesions on card sorting. *Arch. Neurol.* **9:** 90–100.

Milner, B. 1964. Some effects of frontal lobectomy in man. In *The Frontal Granular Cortex and Behavior* (J. M. Warren and K. Akert, Eds.), pp. 313–334. McGraw–Hill, New York.

Nagahama, Y., Fukuyama, H., Yamauchi, H., Matsuzaki, S., Konishi, J., Shibasaki, H., and Kimura, J. 1996. Cerebral activation during performance of a card sorting test. *Brain* **119:** 1667–1675.

Noll, D. C., Cohen, J. D., Meyer, C. H., and Schneider, W. 1995. Spiral K-space MR imaging of cortical activation. *J. Magn. Reson. Imaging* **5:** 49–56.

Osherson, D., Perani, D., Cappa, S., Schnur, T., Grassi, F., and Fazio, F. 1998. Distinct brain loci in deductive versus probabilistic reasoning. *Neuropsychologia* **36:** 369–376.

Owen, A. M., Downes, J. J., Sahakian, B. J., Polkey, C. E., and Robbins, T. W. 1990. Planning and spatial working memory following frontal lobe lesions in man. *Neuropsychologia* **28:** 1021–1034.

Owen, A. M., Doyon, J., Petrides, M., and Evans, A. 1996. Planning and spatial working memory: A positron emission tomography in humans. *Eur. J. Neurosci.* **8:** 353–364.

Petty, R. G., Bonner, D., Mouratoglou, V., and Silverman, M. 1996. Acute frontal lobe syndrome and dyscontrol associated with bilateral caudate nucleus infarctions. *Br. J. Psychiatry* **168:** 237–240.

Prabhakaran, V., Smith, J. A., Desmond, J. E., Glover, G. H., and Gabrieli, J. D. 1997. Neural substrates of fluid reasoning: An fMRI study of neocortical activation during performance of the Raven's Progressive Matrices Test. *Cognit. Psychol.* **33:** 43–63.

Prabhakaran, V., Rypma, B., and Gabrieli, J. D. E. 2001. Neural correlates of mathematical reasoning: An fMRI study of neocortical activation during performance of the Necessary Arithmetic Operations Test. *Neuropsychology* **15:** 115–127.

Ragland, J. D., Gur, R. C., Glahn, D. C., Censits, D. M., Smith, R. J., Lazarev, M. G., Alavi, A., and Gur, R. E. 1998. Frontotemporal cerebral blood flow change during executive and declarative memory tasks in schizophrenia: A positron emission tomography study. *Neuropsychology* **12:** 399–413.

Raichle, M. E. 1998. The neural correlates of consciousness: An analysis of cognitive skill learning. *Philos. Trans. R. Soc. London B Biol. Sci.* **353:** 1889–1901.

Raichle, M. E., MacLeod, A. M., Snyder, A. Z., Powers, W. J., Gusnard, D. A., and Shulman, G. L. 2001. A default mode of brain function. *Proc. Natl. Acad. Sci. USA* **98:** 676–682.

Rao, S. M., Bobholz, J. A., Hammeke, T. A., Rosen, A. C., Woodley, S. J., Cunningham, J. M., Cox, R. W., Stein, E. A., and Binder, J. R. 1997. Functional MRI evidence for subcortical participation in conceptual reasoning skills. *NeuroReport* **8:** 1987–1993.

Raven, J. C. 1938. Standardization of progressive matrices. *Br. J. Med. Psychol.* **19:** 137–150.

Robin, N., and Holyoak, K. J. 1995. Relational complexity and the functions of prefrontal cortex. In *The Cognitive Neurosciences*

(M. S. Gazzaniga, Ed.), 1st ed., pp. 987–997. MIT Press, Cambridge, MA.

Singh, J., Gabrieli, J. D. E., and Goetz, C. G. 1992. Impairment of working memory in patients with Huntington's disease. *Neurology* **42:** 280.

Shallice, T., and Burgess, P. W. 1991. Higher-order cognitive impairments and frontal lobe lesions in man. In *Frontal Lobe Function and Dysfunction* (H. S. Levin, H. M. Eisenberg, and A. L. Benton, Eds.), pp. 125–138. Oxford Univ. Press, New York.

Shallice, T., Fletcher, P., Frith, C. D., Grasby, P., Frackowiak, R. S. J., and Dolan, R. J. 1994. Brain regions associated with acquisition and retrieval of verbal episodic memory. *Nature* **368:** 633–635.

Talairach, J., and Tournoux, P. 1988. *Co-planar Stereotaxic Atlas of the Human Brain.* Thieme, Stuttgart/New York.

Tomasello, M., and Call, J. 1997. *Primate Cognition.* Oxford Univ. Press, New York.

Van den Bercken, J. H. L., and Cools, A. R. 1982. Evidence for a role of the caudate nucleus in the sequential organization of behavior. *Behav. Brain Res.* **4:** 319–337.

Vazquez, A. L., and Noll, D. C. 1998. Nonlinear aspects of the BOLD response in functional MRI. *NeuroImage* **7:** 108–118.

Waltz, J. A., Knowlton, B. J., Holyoak, K. J., Boone, K. B., Mishkin, F. S., de Menezes Santos, M., Thomas, C. R., and Miller, B. L. 1999. A system for relational reasoning in human prefrontal cortex. *Psychol. Sci.* **10:** 119–125.

Wharton, C. M., Grafman, J., Flitman, S. S., Hansen, E. K., Brauner, J., Marks, A., and Honda, M. 2000. Toward neuroanatomical models of analogy: A positron emission tomography study of analogical mapping. *Cognit. Psychol.* **40:** 173–197.